Symmetry and Stability of Solitary Dimer Rows on Si(100)

P. Bedrossian[(1)] and Efthimios Kaxiras[(2)]

[(1)]*Lawrence Livermore Laboratory, P.O. Box 808, L-350, Livermore, California 94550*

[(2)]*Department of Physics and Division of Applied Sciences, Harvard University, Cambridge, Massachusetts 02138*

(Received 8 October 1992)

Metastable, monolayer-high structures as narrow as one dimer row and as long as the substrate's terrace width decorate antiphase boundaries on Si(100) following 225 eV Xe bombardment. On the basis of tunneling microscope observations and first-principles calculations, we propose that the bonding topology of a buckled dimer row on an antiphase boundary is responsible for the metastability of this "zipper" structure, and in turn for the preferential nucleation of dimer rows on antiphase boundaries during growth.

PACS numbers: 68.35.Bs, 68.55.Jk

Experimental and theoretical efforts to understand the complex, nonequilibrium phenomenon of growth have focused increasingly on its microscopic aspects. A realistic description of growth is essential to controlling and improving technologically important processes. For example, the growth of smooth surfaces is a prerequisite for creating sharp, heteroepitaxial interfaces. While much recent effort has considered generalized statistics of island formation and growth roughening [1-3], comparatively little work has addressed the microscopic interactions which underly the nucleation process itself on a real surface, such as Si(100).

Here we demonstrate a novel approach to studying a crucial part of this process by examining the topology and stability of single dimer rows on Si(100), whence any island growth on that surface must originate. While the dimer structure of Si(100) is well established [4,5], the search for the precise bonding topology of atoms on that surface has recently generated intense theoretical and experimental activity. It appears that charge transfer within a single dimer can give rise to a topographic asymmetry, or "buckling," which may be either static or dynamic (oscillating) [6-11]. Arguments in favor of symmetric dimers, without buckling, have also been presented [12,13]. Scanning tunneling microscopy (STM) has observed the buckling of dimers in the vicinity of defects, such as step edges [14,15]. Still, the reason for the observed, defect-induced buckling is not definitively understood. Here we present what we believe to be the first study, employing both STM and first-principles calculations, of the topology and stability of a specific, novel defect on Si(100), the isolated, solitary dimer row. This defect is, in a structural sense, the elementary excitation responsible for island growth on this surface; its study is therefore of fundamental interest.

Single dimer rows on Si(100) can be prepared with lengths limited only by the substrate's terrace width, either by 225 eV Xe bombardment at $T > 450\,^\circ\mathrm{C}$, or by irradiation at lower temperatures followed by annealing at $T > 600\,^\circ\mathrm{C}$. We find that the long dimer chains created under these conditions sit atop antiphase boundaries (APBs), and that the dimers within these chains buckle in a consistent geometry with respect to antiphase domains on either side. Significantly, this "zipper" geometry is metastable; its elimination requires substrate temperatures above 700 °C.

The experiments were performed in an ultrahigh vacuum chamber with base pressure below 10^{-10} torr. The apparatus and sample preparation have been described elsewhere [16,17]. Our preparation does not yield antiphase boundaries on a clean surface. In this work, Si(100) samples held at elevated temperature were exposed to 225 eV Xe bombardment and then quenched to room temperature for imaging by STM. An infrared pyrometer was used to measure sample temperatures during both sputtering and subsequent annealing sequences.

We have previously observed that both Si(111) [16] and Si(100) [17,18] can be sputtered in a layer-by-layer fashion by 225 eV Xe, and that the structural evolution of these surfaces during sputtering is mediated by mobile surface vacancies, which can annihilate at step edges or nucleate monolayer-deep depressions, or "vacancy islands." We now consider the removal of more than a full monolayer. As vacancy islands nucleate and grow, the dimer rows in separate vacancy islands need not, in general, align to each other. An APB will result if two growing vacancy islands meet, but their internal dimer rows are not aligned. We shall find that metastable, lone dimer rows decorate these boundaries.

Figure 1(a) shows such isolated dimer rows on a flat terrace following removal of ≈ 2 monolayers (ML) at 500 °C. The scale of the image testifies to the attainable length of single dimer rows on a suitably flat surface. On a surface with shorter terraces, single dimer strings can span a terrace, as in Fig. 1(b), which was acquired after removal of ≈ 1 ML at 430 °C. Both defects labeled L have width one dimer row; the one on terrace A consists of a single dimer row interrupted by two, small vacancy islands. The detail in Fig. 1(c) shows the misalignment of dimer rows on opposite sides of the defect, which partitions the terrace. Most of the islands in the next higher terrace, labeled B in Fig. 1(b), also sit on APBs, and some are as narrow as a single dimer row. These structures are stable up to 710 °C.

© 1993 The American Physical Society

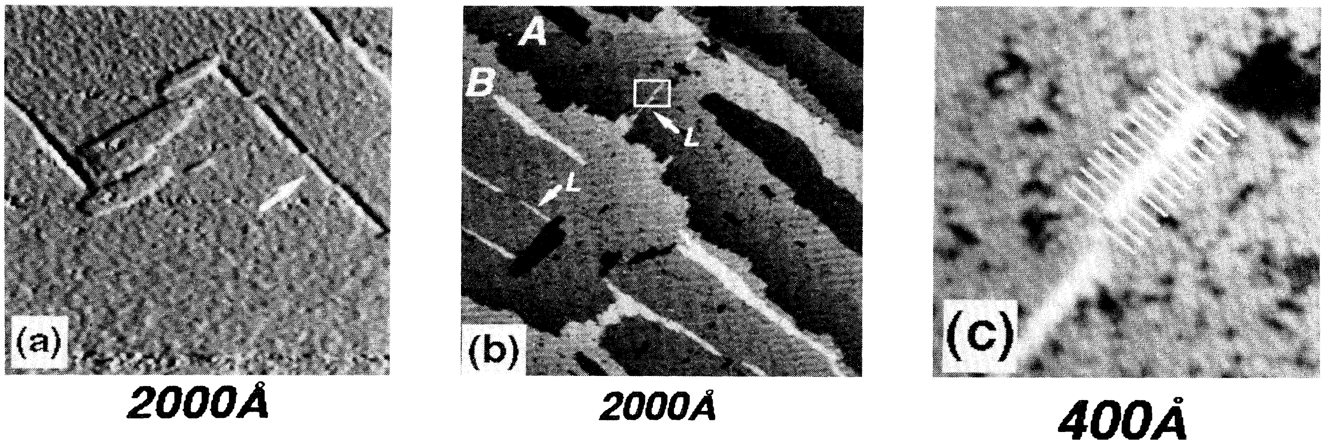

FIG. 1. (a) 2000 Å STM image of Si(100) showing long dimer strings after removal of ≈ 2 ML by 225 eV Xe sputtering. In this and subsequent images, the tip bias is +1.7 V, and the tunneling current is 0.7 nA. (b) 2000 Å image following removal of ≈ 1 ML from a surface misoriented 1/4° towards the [110] direction. The defects labeled L are islands of width one dimer. (c) 400 Å detail the antiphase defect in the boxed region in (b). The dimer rows on either side of the raised island do not line up.

We have investigated the formation of such decorated APBs further by separating the sputtering and annealing steps, i.e., annealing surfaces initially sputtered at lower temperature and ion fluence. Figure 2(a) shows a surface after sputter removal of ≈ 1/4 ML at 350 °C. Despite the nucleation of a high density of small vacancy islands, the overall step structure of the starting surface is still apparent, and no long islands have formed at this stage. However, after annealing at 500 °C for 6 min and 650 °C for 2 min, narrow islands and peninsulas partition the surface into antiphase domains. Because the high density of antiphase domains in Fig. 2(b) did not appear in Fig. 2(a), these domains must have formed from the coalescence of smaller vacancy islands in Fig. 2(a) during the annealing step. After annealing, we observe the long, narrow islands only on APBs. The absence of an analogous defect without an APB suggests that only the antiphase defect is stable at the temperatures under consideration. A temperature of 710 °C was required to heal these defects and recover a surface with evenly distributed steps.

Closer examination of one narrow island in Fig. 2(c) reveals that it is buckled such that the incoming dimer rows on the lower terrace on either side are terminated by the brighter atom of each dimer pair on the island. This image, acquired with positive tip bias, probes occupied sample states. Therefore, the brighter spot in the image corresponds to an almost fully occupied dangling bond orbital associated with the higher atom in the buckled dimer. [See also theoretical treatment below and accom-

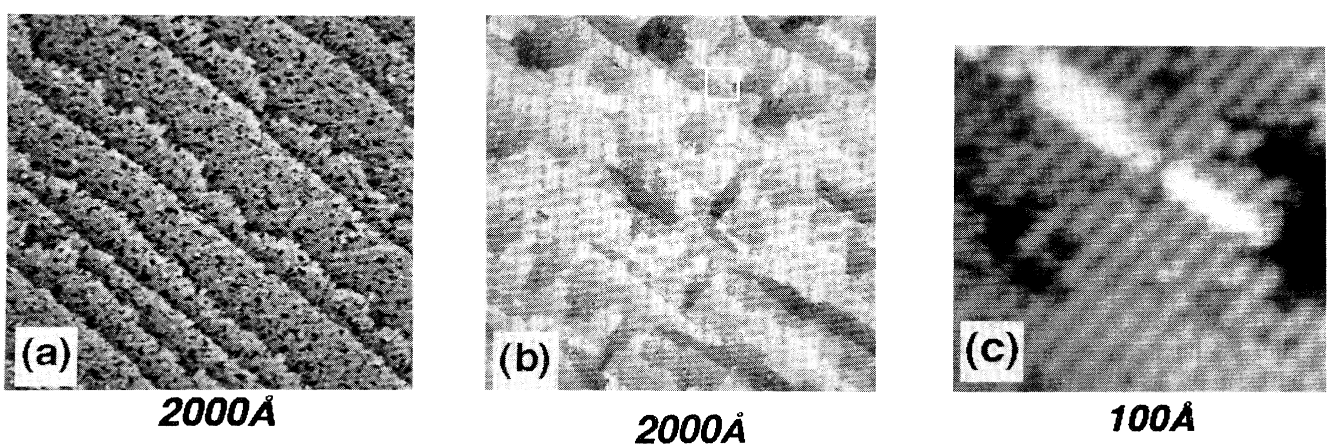

FIG. 2. (a) 2000 Å image following removal of ≈ 1/4 ML by 225 eV Xe sputtering, showing a high density of small vacancy islands. (b) 2000 Å image following annealing of the surface in (a) at 500 and 650 °C (see text). (c) 100 Å detail of the boxed region in (b), showing the buckling topology of the antiphase defect.

panying Figs. 3(b) and 4(b)].

The last observation is consistent with the previous report that when the upper terrace of a monatomic step is terminated by a straight dimer row, then that row is buckled, the orientation of the buckling alternates on adjacent dimers, and the incoming dimers on the lower terrace terminate on raised atoms of the buckled row [14]. Since each side of the single-row defect is a monatomic step, its formation on an APB allows each side to terminate the surrounding dimer rows in a manner consistent with the single-step termination. Our observation that decorated antiphase defects terminate at terrace or vacancy island ledges [Figs. 1(a)–1(c) and 2(b) and 2(c)] is consistent with the previous report that antiphase defects on vicinal Si(100) surfaces lead to "kissing sites" that pin meandering steps at terrace ledges [19].

In order to investigate the stability of single dimer rows in the absence or presence of APBs, we have calculated the relative energy and atomic relaxation of two configurations: (i) a single dimer row on an otherwise perfect Si(100)-2×1 surface (no APB), and (ii) a dimer row on staggered rows of dimers (APB present). We have used first-principles calculations based on the local density approximation to density functional theory and atomic pseudopotentials to eliminate the Si core electrons. The two configurations were fully relaxed by minimizing the calculated Hellmann-Feynman forces [20]. As shown in Fig. 3, the presence of an APB [Fig. 3(b)] leads to pronounced buckling of the dimers of the single, elevated row. By contrast, in the absence of APBs, [Fig. 3(a)], the dimers of the single row are at two distinct heights, but they are symmetrical: dimers that fall between the substrate dimers (crests) are elevated, whereas dimers that fall outside the substrate dimers (troughs) are depressed. The relaxation in the two configurations reveals an intricate balance of strain between the dimers on the single row and those of the substrate.

We find that configuration (ii) is lower in energy than (i) by 0.4 eV per dimer along the solitary, elevated row. This energy difference results from the optimal atomic relaxation for the individual dimers, which is achieved only in the presence of the APB. The asymmetric strain field produced by the staggering of dimer rows on either side of the APB causes the two atoms in each dimer of the elevated row to experience opposite forces, enhancing and stabilizing the buckling of dimers on the single row. The compressive strain at the end point of a substrate dimer row forces the adjacent atom of the elevated row to buckle up. Conversely, the tensile strain between two substrate dimers forces the adjacent atom of the elevated row to buckle down. In the absence of the APB, the two atoms in any one dimer in the solitary row experience a symmetric strain, so buckling is prohibited; alternate dimers along the row experience opposite strain, which produces an undulation in dimer height. This higher-energy geometry is *not* seen in the STM images [21].

For a more direct comparison with the STM observations, we present in Figs. 4(a) and 4(b) the electronic densities, at fixed height, using the calculated wave func-

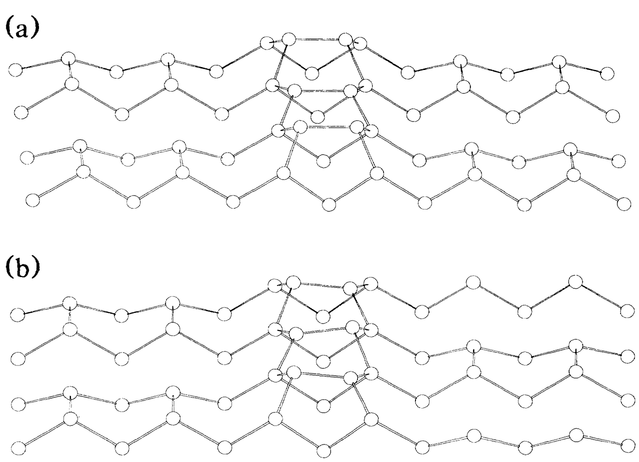

FIG. 3. Calculated relaxed geometries, shown in perspective, for a solitary, elevated dimer row on (a) a defect-free substrate, and (b) an antiphase boundary (APB).

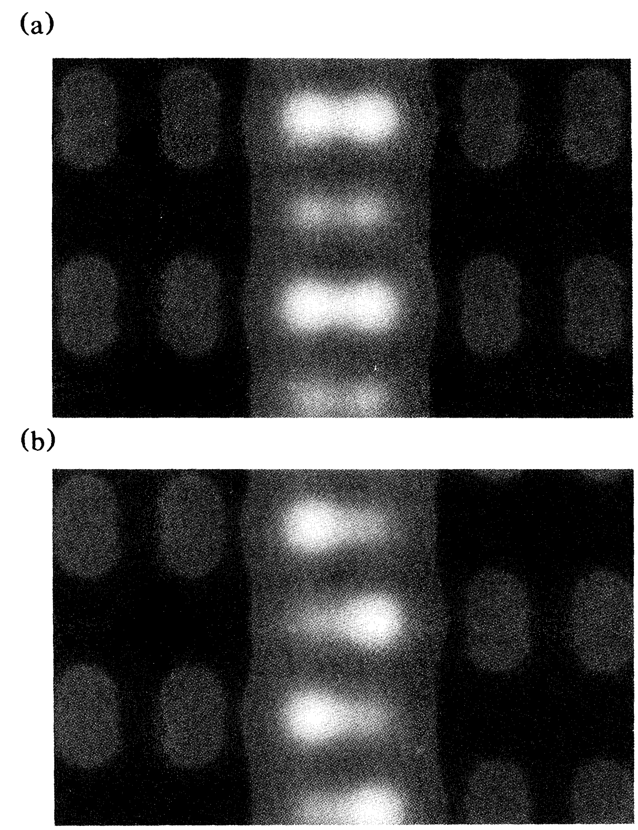

FIG. 4. Density contours corresponding to occupied electronic states for the geometries showing Figs. 3(a) and 3(b); brighter shading indicates higher electron density.

tions for the geometries corresponding to Figs. 3(a) and 3(b), respectively. The lowest energy configuration [Fig. 3(b)] produces a charge density consistent with the STM image [compare Fig. 4(b) with Fig. 2(c)]. The higher-energy configuration [Fig. 3(a)] produces a charge density [Fig. 4(a)] which is incompatible with our STM images.

Antiphase boundaries also arise during Si homoepitaxy when islands which nucleate independently grow and meet. It was observed previously that under growth conditions, shorter dimer rows which nucleate on islands do so preferentially on antiphase boundaries [22,23]. This result is consistent with our finding that an individual, buckled dimer row is stabilized by its geometry on an APB relative to a single dimer row on a perfect substrate. Nucleation at an arbitrary site, without any antiphase defect, would therefore be less favorable.

In order to achieve smooth, epitaxial growth for sharp interfaces, it is necessary to suppress the nucleation of successive islands upon islands. The widespread practice of growing Si epitaxially with substrate temperatures about 700 °C [24] is consistent with our observation that such temperatures are necessary to eliminate the zipper defect which we described here.

In conclusion, we have studied long, isolated dimer rows as a model system for both defect-induced dimer buckling and as the elementary excitation, in a structural sense, for island formation. We find that the two issues are closely related, for the bonding topology of a lone dimer row stabilizes a "zipper" defect, consisting of an individual, buckled dimer row atop an antiphase boundary. The high temperature ($\approx 700\,^\circ$C) required to heal this defect implies a fundamental lower limit on the temperature at which sharp interfaces can be created with conventional Si epitaxy.

The authors are grateful to E. Chason, P. Feibelman, J. E. Houston, J. Klepeis, T. Klitsner, C. Mailhiot, T. Michalske, and S. T. Picraux for helpful discussions, and to R. Boatman, D. Buller, G. Fowler, and M. Thomas for technical advice. Work was performed at Sandia National Laboratories, Albuquerque, under the auspices of the U.S. Department of Energy through BES, Office of Materials Science, under Contract No. DE-AC04-76DP00789, and at Lawrence Livermore National Laboratory under Contract No. W-7405-Eng-48. Calculations were performed at the Cornell National Supercomputer Facility. One of us (E.K.) acknowledges the support of the Office of Naval Research, Contract No. N00014-92-J-1138.

[1] S. das Sarma and P. Tamborenea, Phys. Rev. Lett. **66**, 325 (1991).
[2] E. Chason and J. Tsao, Surf. Sci. **234**, 361 (1990).
[3] Y. Mo, R. Kariotis, D. Savage, and M. Lagally, Surf. Sci. **219**, L551 (1989); also Phys. Rev. Lett. **63**, 2393 (1989).
[4] R. Schlier and H. Farnsworth, J. Chem. Phys. **30**, 917 (1959).
[5] R. Tromp, R. Hamers, and J. Demuth, Phys. Rev. Lett. **55**, 1303 (1985).
[6] D. Chadi, Phys. Rev. Lett. **43**, 43 (1979).
[7] F. Jona *et al.*, J. Phys. C **12**, L455 (1979).
[8] M. Yin and M. Cohen, Phys. Rev. B **24**, 2303 (1981).
[9] M. Payne, N. Roberts, R. Needs, M. Needels, and J. Joannopoulos, Surf. Sci. **211/212**, 1 (1989); also Surf. Sci. **236**, 112 (1990).
[10] D. Lin, T. Miller, and T.-C. Chiang, Phys. Rev. Lett. **67**, 2187 (1991).
[11] J. Dabrowski and M. Scheffler, Appl. Surf. Sci. **56**, 15 (1992).
[12] E. Artacho and F. Yndurain, Phys. Rev. Lett. **62**, 2491 (1989).
[13] I. Batra, Phys. Rev. B **41**, 5048 (1990).
[14] R. Hamers, R. Tromp, and J. Demuth, Phys. Rev. B **34**, 1388 (1986).
[15] R. Wolkow, Phys. Rev. Lett. **68**, 2636 (1992).
[16] P. Bedrossian and T. Klitsner, Phys. Rev. B **44**, 13783 (1991).
[17] P. Bedrossian and T. Klitsner, Phys. Rev. Lett. **68**, 646 (1992).
[18] P. Bedrossian, J. E. Houston, E. Chason, J. Y. Tsao, and S. T. Picraux, Phys. Rev. Lett. **67**, 124 (1991).
[19] B. Swartzentruber, Y. Mo, and M. Lagally, Appl. Phys. Lett. **58**, 822 (1991).
[20] We use a plane-wave basis with kinetic energy up to 7.5 Ry, 6 points in the irreducible Brillouin zone, and allow three layers of the substrate to relax, in addition to the single, elevated dimer. The surface unit cell has dimensions (2×4), in conventional units, for configuration (i) and $c(2\times8)$ for configuration (ii).
[21] In the context of our analysis, one cannot compare directly the energies of a solitary dimer row on an APB with either a defect-free 2×1 surface or a bare APB, because each configuration contains a different number of atoms; hence, a chemical potential is implied.
[22] R. Hamers, U. Köhler, and J. Demuth, Ultramicroscopy **31**, 10 (1989).
[23] A. Rockett, Surf. Sci. **227**, 208 (1990).
[24] F. Allen, Thin Solid Films **123**, 273 (1985).

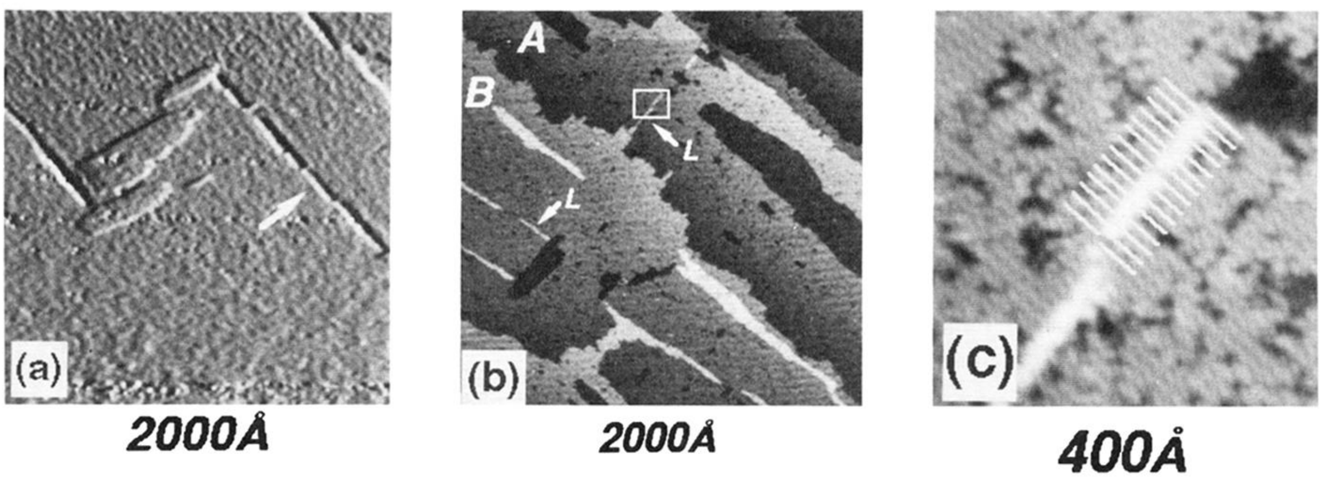

FIG. 1. (a) 2000 Å STM image of Si(100) showing long dimer strings after removal of ≈ 2 ML by 225 eV Xe sputtering. In this and subsequent images, the tip bias is $+1.7$ V, and the tunneling current is 0.7 nA. (b) 2000 Å image following removal of ≈ 1 ML from a surface misoriented 1/4° towards the [110] direction. The defects labeled L are islands of width one dimer. (c) 400 Å detail the antiphase defect in the boxed region in (b). The dimer rows on either side of the raised island do not line up.

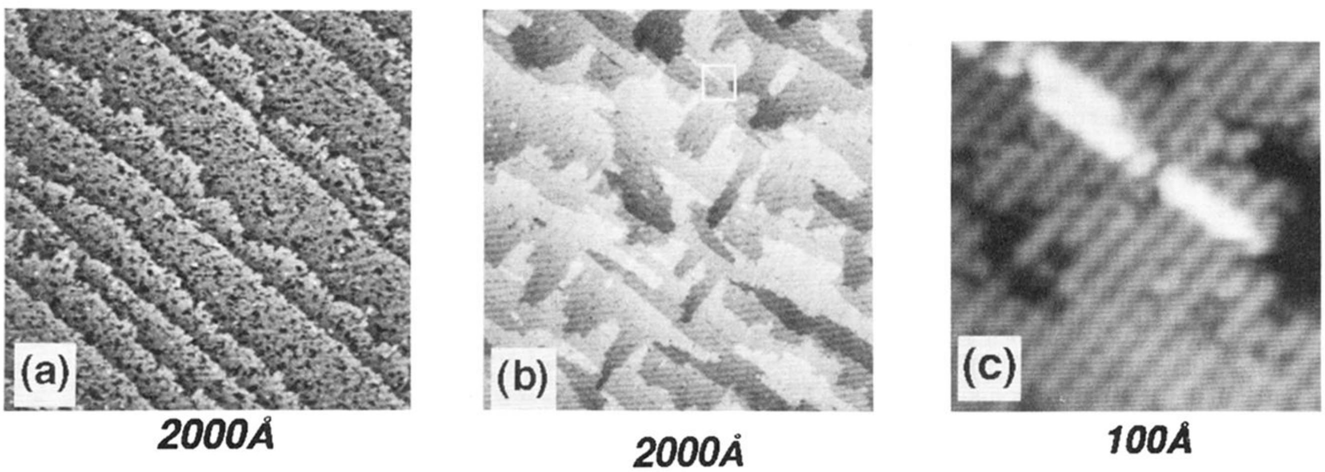

FIG. 2. (a) 2000 Å image following removal of ≈ 1/4 ML by 225 eV Xe sputtering, showing a high density of small vacancy islands. (b) 2000 Å image following annealing of the surface in (a) at 500 and 650 °C (see text). (c) 100 Å detail of the boxed region in (b), showing the buckling topology of the antiphase defect.

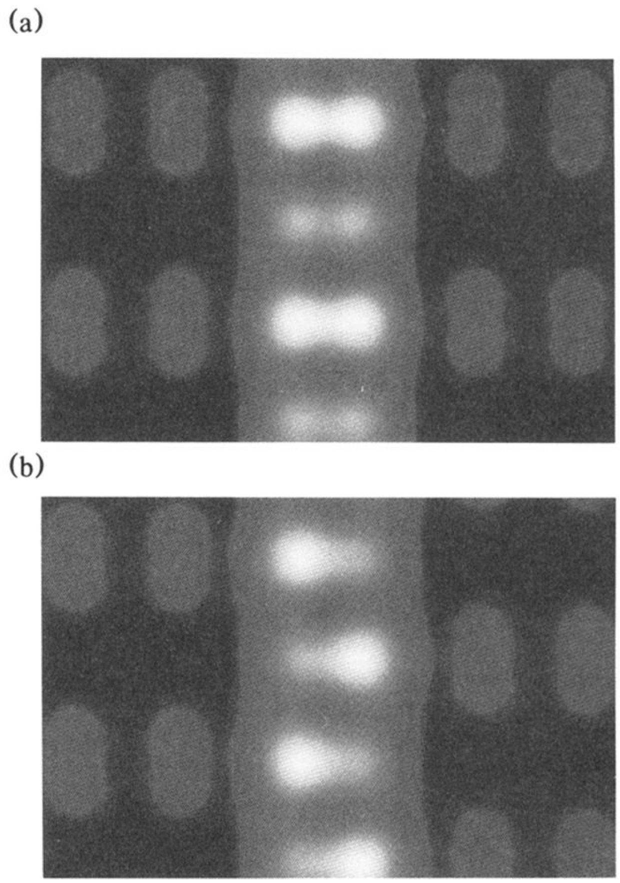

FIG. 4. Density contours corresponding to occupied electronic states for the geometries showing Figs. 3(a) and 3(b); brighter shading indicates higher electron density.